Commissioning of the S^3 Stable Targets' Station

Christelle Stodel, Franck Lutton, Patrice Gangnant, Thierry Lefrou, Charles Houarner, Thierry André, Georges Frémont, Marius Bourges, Franck Saillenfest, Vincent Morel, et al.

Commissioning of the S^3 Stable Targets' Station

Christelle Stodel[1*], *Franck* Lutton[1], *Patrice* Gangnant[1], *Thierry* Lefrou[1], *Charles* Houarner[1], *Thierry* André[1], *Georges* Frémont[1], *Marius* Bourges[1], *Franck* Saillenfest[1], *Vincent* Morel[1], *Julien* Piot[1], *Dieter* Ackermann[1], *Hervé* Savajols[1], *Gilles* de France[1], *Shayan* Kumar[1], *Bertrand* Jacquot[1], *Omar* Kamalou[1], *Xavier* Ledoux[1], and *Olivier* Sorlin[1], on behalf of the S^3 Collaboration

[1]Grand Accélérateur National d'Ions Lourds (GANIL), CNRS/IN2P3-CEA/DRF, Bd Henri Becquerel, 14076 Caen, France

Abstract. In order to handle the very intense heavy ion beams from the GANIL-SPIRAL2 superconducting linear accelerator (LINAG), a specific target station for stable material was designed and built upstream of the Super-Separator-Spectrometer S^3. After testing separately all components of this station, the whole system was evaluated under realistic irradiation conditions. This paper reports on the specifications of the set-up and the results of the test.

1 Introduction

The roadmap for many of today's nuclear accelerator facilities is based on the study of rare events in nuclear and atomic physics. Indeed, by reaching and studying increasingly exotic nuclei, we are contributing to the development of a comprehensive model of atomic nuclei and the understanding of the origin of elements. In the Segré chart, the regions of nuclei above Z = 104, known as super-heavy elements, or at the proton dripline at N=Z, are of particular interest for these investigations. Nevertheless, their production can only be achieved by a fusion-evaporation reaction with a cross-section down to the tenth of picobarn level. Given also their short lifetime, advanced and highly sensitive techniques must be employed to optimize the yield and measurement accuracy of identified nuclei. These requirements are met at GANIL's facilities, with LINAG delivering intense beams to the S^3 installation, which comprises a high-power target station, a multi-stage multi-purpose separator [1] and advanced detection devices [2] [3]. In this paper, the S^3 Stable Targets' Station, will be detailed and its commissioning will be described.

2 Design, fabrication and components of the S^3 Stable Targets' Station

2.1 Specifications (or requirements)

The experimental program at S^3 focuses on the synthesis and study of exotic nuclei produced by fusion-evaporation reactions, in each case using an intense heavy ion (HI) beam and the target material. With LINAG, heavy ion beams reaching 10^{13}-10^{14} pps are achievable with energies of up to 14.5 MeV/u. To optimize the transmission through S^3, their spatial distribution at the target focal point is defined as a double Gaussian with a standard deviation of 0.5 and 2.5 mm in horizontal and vertical direction respectively [1]. Depending on the nuclei of interest, a wide variety of target material is required, with thicknesses ranging from a few tens of µg/cm² to a few mg/cm². In general, the limiting factors for targets are their degradation due to radiation damage and heating, which can induce mechanical stress and melting if the fusion temperature is reached. In the case of stable material, i.e. no radioactive species, fusion temperature can be as low as a few hundred °C, for instance 271,4 °C for bismuth. Due to their thinness and working conditions under vacuum, the main process of cooling is radiation through the surfaces of the target foils. To prevent overheating of the material, the beam is distributed over a large target area by mounting them on a rotating wheel. The latter was designed with a radius at the beam impact of 335 mm and for a rotation velocity up to 3000 rpm [4]. In order to optimise the transmission of the nuclei of interest through S^3, a second wheel with identical dimensions holding thin carbon foils which equilibrates the charge of the recoiling ion, is needed behind the target wheel. Moreover, in order to monitor the target integrity and the beam characteristics, i.e., beam spot profile, intensity and time structure, the vacuum irradiation chamber is equipped with a variety of instrumentation.

2.2 Mechanical parts and its motorization

The S^{4}TS, acronym for S^3 Stable Targets' Station, consists of a compact vacuum chamber 404 mm wide, 1,000 mm high and 816 mm in diameter.

* Corresponding author: christelle.stodel@ganil.fr

The two wheels have an external diameter of 743 mm corresponding to a 670 mm diameter at the beam impact and are spaced 100 mm part.

Each wheel can support six sectors fixed with eccentric clams and three target frames can be mounted on each sector, as illustrated on Fig. 1.

The design of the frames was optimized in order to prevent the mechanical buckling under high rotation and to increase the irradiation surface according to the beam spot size. Their aperture dimensions are 108.9 mm large and 19.7 mm or 30 mm high corresponding to surfaces of 21,5 cm² and 32,7 cm² for the targets and charge equilibrium foils respectively. The length of one target with its frame at the beam impact radius is 116.9 mm.

Fig. 1. View inside the chamber of the two wheels with their respective six sectors and targets or charge equilibration carbon foils mounted.

The two wheels are mounted on a common axle and are driven through a ferrofluidic feed through by a servo-motor (Maxon EC60). Through a drive belt, a 13-bit encoder provides the absolute position of the wheel with an accuracy better than 1 mrad corresponding to 257 µm at the beam impact position.

The motor and the reading of its absolute encoder value are controlled by a National Compact RIO controller via a LabVIEW interface. This system enables generating some user defined signals (TTL): a first one for each revolution of the wheel and a second one with a time structure corresponding to the widths of target segments requested to be irradiated.

In addition, a hall probe and an optical switch sensor are positioned on a small tooth wheel (18 teeth) fixed on the rotating arm (Fig. 2). The hall probe produces a signal for each revolution, redundant to the one described above with the encoder. The optical sensor sets up 18 equi-distant TTL signals along one revolution.

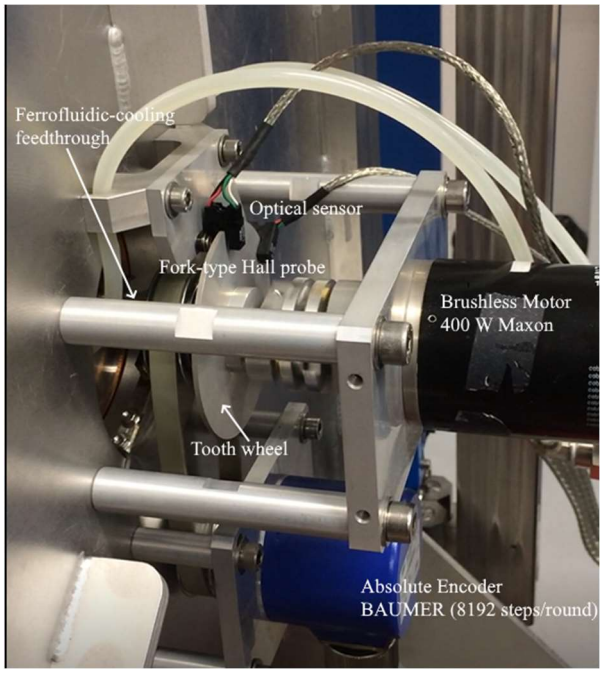

Fig. 2. Motorisation set-up

2.3 Beam control equipment

A Secondary Emission Monitor (SEM) profiler [5] can be inserted along the beam axis upstream the first wheel. With its horizontal and vertical 47 wires spaced by 0.5 mm, the beam profile can be evaluated. A few centimetres downstream, a Faraday Cup can be inserted and used to protect the targets during beam tuning at low intensity, limited to 30 W (Fig. 3).

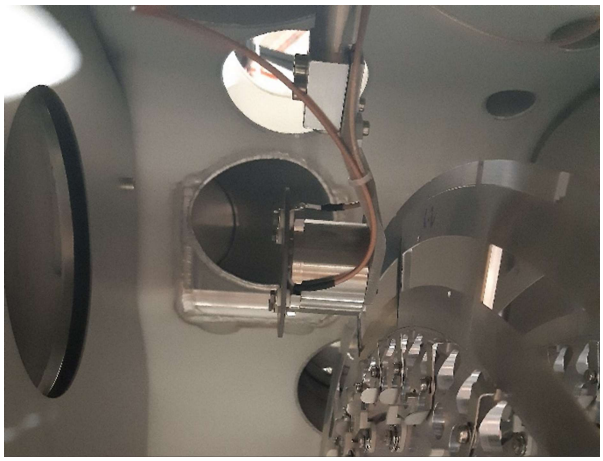

Fig. 3. View of the Faraday Cup for the HI beam.

Outside the station, a BaF_2 (barium fluoride) scintillator, sensitive to gamma radiation emitted by the interaction of the beam with the frames or the target material is positioned at about 1.5 m from the interaction point. This detector is shielded by lead to reduce the gamma-ray background from any external source.

2.4 Targets integrity Detectors

The integrity of targets mounted on the upstream wheel are monitored by three methods: alpha particle energy loss, particle scattering and transmission of an electron

beam. The working principle and the systems are described in [6][7] and shown in **Fig. 4** and Fig. 5.

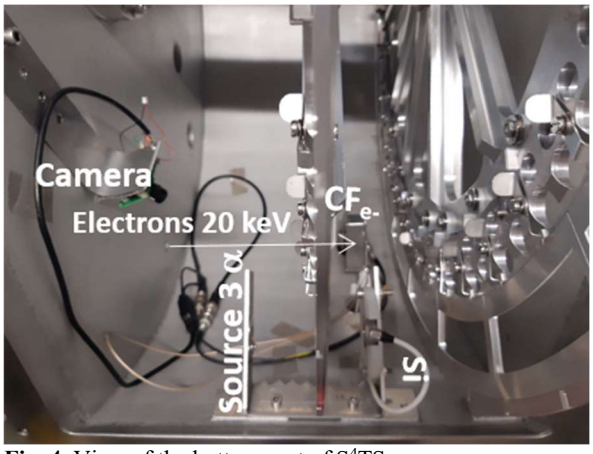

Fig. 4. View of the bottom part of S[4]TS

In contrast to the electron gun from GSI [8] used in [7], the S[4]TS is equipped with an electron gun EH-30-3 from STAIB Instruments. Its control and command was developed at GANIL to remotely configure the energy and intensity of the electron beam and the deflection sequence according to the wheel rotation signal with a LabVIEW application and a customized signal processing. The deflector allows a radial scan of the target to obtain a full image of its surface with a position resolution of 0.5 mm. In addition, a current/voltage converter was designed to measure the electron current output signal from the Faraday cup, CFe- on **Fig. 4**.

Fig. 5. View of the upper part of S[4]TS with the scattered particles detectors, sectors of the first wheel are removed

To measure scattered particles of the beam or target particles, two silicon detectors can be inserted at two different position downstream the target wheel, Fig. 5. The distance and angle between the centre of the silicon and the beam impact on the target are displayed on Table 1. To limit the counting rate of the detectors, they are protected with a rotating brass collimator with a hole of 1 mm diameter spaced at 5 mm from the centre of the silicon detectors.

Table 1. Setting of scattered detectors.

Stroke of insertion	Silicon N°	Distance Target/center Si (mm)	Angle (°)
1	Si 1	82.0	58.4
	Si 2	75.5	31.9
2	Si 1	76.2	43.4
	Si 2	78.2	20.9

2.5 Data acquisition

All the signals, i.e. from the silicon detectors, the BaF2 scintillator, the electron Faraday cup and the deflector, the wheel rotation, are processed, digitalized. All events are time-stamped with a 10 ns granularity for a depth of 48 bits by a dedicated NUMEXO2 (NUMériseur pour EXOgam2) NIM digitizer. The data obtained make it possible to display the various observables, either their count rate or their energy, along the targets.

3 Validation under irradiation

Until 2022, all the components of the target station were developed and tested separately, and it was essential to evaluate the whole system under realistic irradiation conditions. In July 2023, the target station was installed on the LISE2000 beam line. Except the upstream collimators and the SEM profiler inside the S[4]TS, all instrumentation described above were on operation. Upstream the S[4]TS, a SEM profiler was used to control the beam profile, a cooled Faraday Cup was installed downstream the S[4]TS where the beam was dumped.

Sixteen targets of various material and thickness were mounted on the target wheel with thicknesses and positions given on Table 2. Tin, bismuth and ytterbium targets were made by evaporation on a thin carbon backing of about 30 µg/cm², they were covering all the surface of the frames, i.e. 21.2 cm². Thick uranium and terbium targets were made by molecular plating [9] on a thick titanium backing of about 10 µm. As their surface was only few cm², 0.8 cm² of deposition on a square backing of 4 cm², 2 uranium and 3 terbium targets were placed on frames 2.3 and 6.1 respectively.

Table 2. Targets used during the July 2023 test

Material (backing + target)	Thickness (µg/cm²)	Position on the wheel (N°sector-1..3)
C+Sn	≈30 + ≈ 20	4.1; 4.2; 4.3
C+Bi-metal	≈30 + 320	1.1; 1.2; 1.3; 2.1; 6.3
C+Bi-oxyde	≈30 + 340	2.2; 3.1; 3.2;3.3
C+Yb	≈30 + ≈ 400	5.2; 5.3;
Ti+U	4500 + 288	2 on 2.3
Ti+Tb	4500 + 2000	3 on 6.1

A $^{20}Ne^{3+}$ beam at 4.5 MeV/u was delivered for about 48 hours from few nA to 1.8 µA. The total dose was $1.8*10^{14}$ ions. All irradiation periods were performed at a speed of the wheel between 0 to 1000 rpm

3.1 Control of the beam

Firstly, the intensity of the beam stopped in the HI Faraday cup, Fig. 3, was measured with a digital current integrator (ORTEC 439). Its response was observed to be proportional to the intensity obtained with the beam

intensity monitor of the cyclotron (CF44) in the range of intensities corresponding to 1 to 30 watts.

Secondly, the control of the accelerator chopper was checked with the user defined signal described in 2.2. This beam time structure function is essential to avoid irradiating target frames and to optimise irradiation of the effective surface of the material. Because of delays from the electronics and of the tails of the beam distribution in horizontal direction, this time structure has to be adjusted. The count rate of the BaF_2 scintillator at each revolution of the wheel is used to control the synchronisation of the rotation with the temporal structure of the beam and to adjust these parameters, i.e. the start-up time and the width of the signal allowing the beam to reach each target.

Without applying this synchronisation, the targets are irradiated at low intensity (about 100 nAe) and the count rate of the BaF_2 along the revolution is recorded. As expected, we observe on the spectrum that the 18 peaks (Fig. 6) corresponding to the width of the frames between the targets can be identified. The BaF_2 count rate is three times higher than that recorded during the width of the targets. Moreover, a zoom on two consecutive targets placed on two sectors which are not exactly in contact is clearly indicated on Fig. 7.

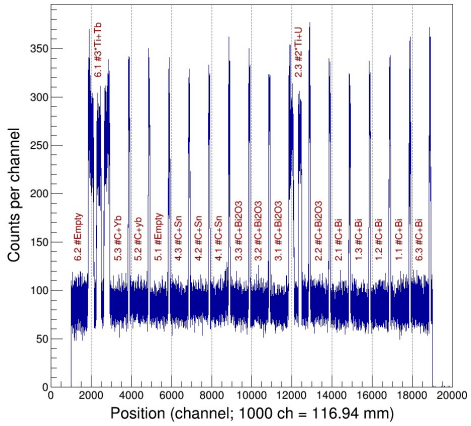

Fig. 6 : Count rate of the BaF_2 along the wheel revolution without synchronisation of the beam with the rotation.

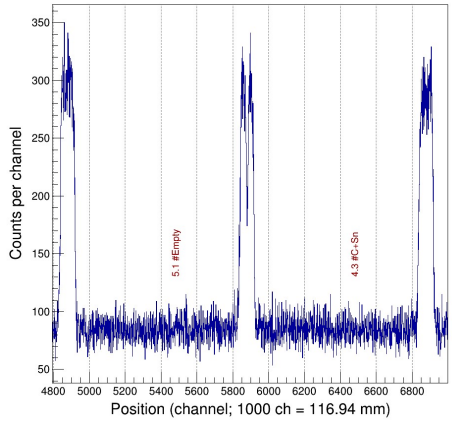

Fig. 7 : Same as **Fig. 6** zoomed on the region of targets 5.1 & 4.3

On Fig. 8, the time structure of the beam was set-up to allow irradiation on each target except on the frames and on the targets 4.3 and 6.2. Moreover, for target 5.1, the irradiation length was reduced to 72% of the potential effective length of the target. Because of the thick Ti backing of targets 2.3 and 6.1, the count rate is higher than for the other targets. The count rate on target 5.1 which has no material can be explained either by the vertical width of the beam with a tail impinging on the upper and lower part of the frame or by the Faraday cup placed few meters downstream to stop the beam.

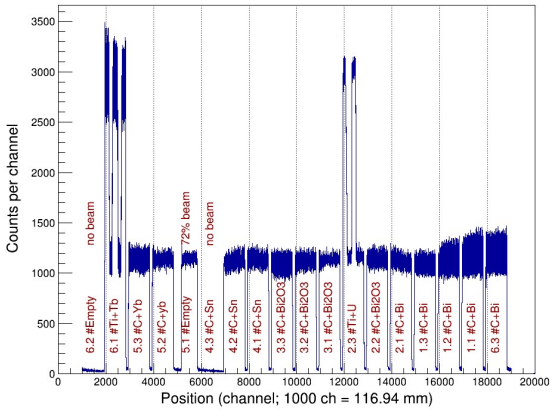

Fig. 8 : Count rate of the BaF_2 along the wheel revolution with synchronisation of the beam with the rotation of the wheel.

3.2 Control of Targets integrity

When the beam intensity is higher, the target material may undergo greater degradation due to the sputtering effect or the increase in temperature. It is therefore essential to monitor their integrity during irradiation and to adjust the beam's temporal structure accordingly if certain parts of the targets are no longer of interest. The detectors described in 2.4 were used during the test to check their relevance and performance.

With the electron-gun tuned at 20 keV and its vertical deflector, a two-dimensional image of the wheel is obtained and displayed on Fig. 9. On can distinguish very thin (green), thick targets (blue) and empty spaces (red). Empty spaces in red correspond to the two frames without any material (6.2 &5.1), the spaces between the 2 and 3 targets of small dimension of Ti +U or Tb on frames 2.3 and 6.1 and the space between each sectors which are not fully joined.

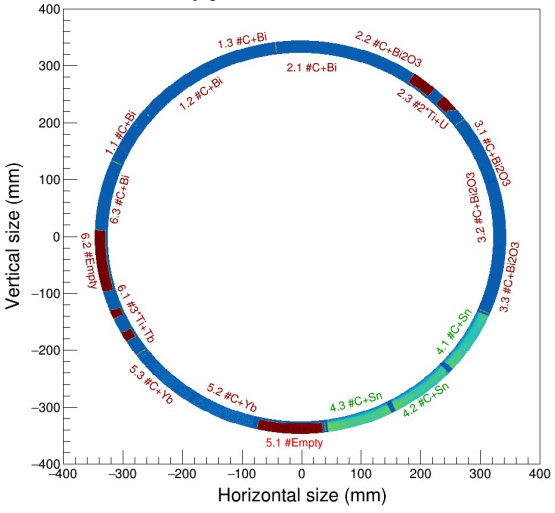

Fig. 9 : Image of the targets with the electron gun

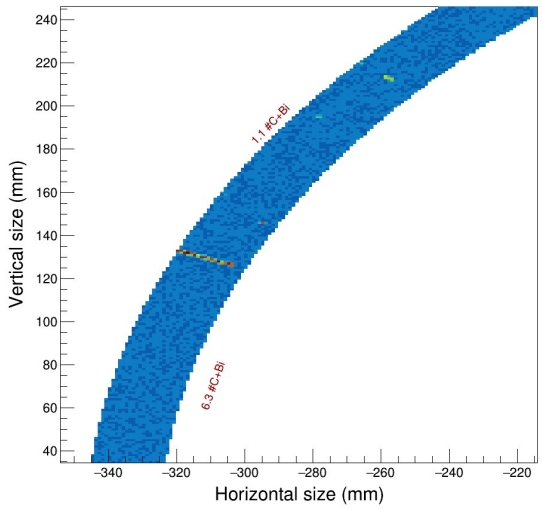

Fig. 10. Zoom on target 1.1

Three small pinholes of less than 1 mm in diameter were made on target 1.1 and are observed on Fig. 10.

After the irradiation, all targets were visually checked and no damage was observed.

4 Conclusion and outlook

In conclusion, with these beam conditions, we were able to validate the response of the heavy ion Faraday cup, the synchronization of the beam with the wheel rotation, the detection systems and the data acquisition. Following the feedback from this test, some feedthroughs have been enlarged and added in the chamber in order to facilitate the access to some connections. In addition, in order to adjust the beam profile on the targets, two carbon collimators of two different aperture surfaces were placed at the entrance of the chamber. They can be inserted independently and for each of them, a beam current can be monitored.

The station has moved to S^3 areas and was commissioned successfully with a LINAG $^{40}Ar^{14+}$ beam at 5 MeV/u in November 2024.

Acknowledgements

The authors would like to thank the GANIL's mechanical design department for designing and following the conception of the targets stations for S^3, the technical groups for improving the electronics set-ups (GGOI and GEF), for producing high quality thin targets (DELPH) and accelerator staff for the high quality of the beam. This work was supported by the Région Basse-Normandie under the CPER (Contrat Plan Etat Région Normandie) 2007–2013 contract and by European Union as regards to European funds for regional development FEDER 2007–2013.

Journal articles

1. F. Déchery, A. Drouart, H. Savajols, J. Nolen, M. Authier, A. M. Amthor, D. Boutin, O. Delferriére, B. Gall, A. Hue, B. Laune, F. Le Blanc, S. Manikonda, J. Payet, M.-H. Stodel et E. Traykov, Toward the drip lines and the superheavy island of stability with the Super Separator Spectrometer S3, Eur. Phys. J. A **51**, 66 (2015)
2. J. Piot, S3: Pushing Spectroscopy Forward, Acta Physica Polonica B **43**, 285 (2012)
3. J. Romans, A. Ajayakumar, M. Authier, F. Boumard, L. Caceres, J.-F. Cam, A. Claessens, S. Damoy, P. Delahaye, P. Desrues, W. Dong, A. Drouart, P. Duchesne, R. Ferrer, X. Fléchard, S. Franchoo, P. Gangnant, S. geldhof, R. P. de Groote, N. Lecesne, R. Leroy, J. Lory, F. Lutton, V. Manea, Y. Merrer, I. Moore, A. Ortiz-Cortes, B. Osmond, J. Piot, O. Pochon, S. Raeder, A. de Roubin, H. Savajols, S. Sels, D. Studer, E. Traykov, J. UUsitalo, C. Vandamme, M. Vendebrouck, P. Van den Bergh, P. Van Duppen et K. Wendt, High-resolution laser system for the S3-Low Energy Branch, Nuclear Inst. and Methods in Physics Research B **536**, 72-81 (2023)
4. C. Stodel, J.-F. Libin, C. Marry, F. Lutton, M.-G. Saint-Laurent, B. Bastin, J. Piot, E. Clément, S. Le Moal, V. Morel, J.-C. Thomas, O. Kamalou, G. Grémont, C. Spitaels, H. Savajols, R. Hue, P. Gangnant, M. Authier, A. Drouart, A. Van Lauwe, E. Lamour, J. Kallunkathariyil, C.-O. Bacri, V. Petitbon-thévenet, H. Lefort et F. Pellemoine, High Intensity targets stations for S3, Journal of Radioanalytical and Nuclear chemistry **305**, 761-767 (2015)
5. J.-L. Vignet, A. Delannoy, E. Guéroult, P. Gangnant, J.-C. Foy, S. Cuzon, C. Houarner et M. Blaizot, The Beam Profile Monitors for SPIRAL 2, Proc. DIPAC'09, paper TUPB07, 176-178, May (2009)
6. C. Stodel, Methods of Targets' Characterization, EPJ Web of conferences **229**, 02001 (2020)
7. J. Kallunkathariyil, C. Stodel, C. Marry, G. Frémont, B. Bastin, J. Piot, E. Clément, S. Le Moal, V. Morel, J.-C. Thomas, O. Kamalou, C. Spitaëls, H. Savajols, M. Vostinar, F. Pellemoine et W. Mittig, S3 Target Monitoring with an Electron gun, AIP Conference Proceedings **1962**, 030019 (2018)
8. R. Mann, D. Ackermann, S. Antalic, H.-G. Burkhardt, P. Cagarda, D. Gembalies-Datz, W. Hartmann, F. P. Hessberger, S. Hofmann, B. Kindler, P. Kuusiniemi, B. Lommel, S. Saro, H. G. Schött et J. Steiner, On-line Target Control, GSI Scientific Report 2003, 224 (2004)
9. E. Artes et, to be published